

## RESEARCH ARTICLE

# Red blood cell carbonic anhydrase mediates oxygen delivery via the Root effect in red drum

Angelina M. Dichiera\* and Andrew J. Esbaugh

## ABSTRACT

Oxygen (O<sub>2</sub>) and carbon dioxide (CO<sub>2</sub>) transport are tightly coupled in many fishes as a result of the presence of Root effect hemoglobins (Hb), whereby reduced pH reduces O<sub>2</sub> binding even at high O<sub>2</sub> tensions. Red blood cell carbonic anhydrase (RBC CA) activity limits the rate of intracellular acidification, yet its role in O<sub>2</sub> delivery has been downplayed. We developed an *in vitro* assay to manipulate RBC CA activity while measuring Hb-O<sub>2</sub> offloading following a physiologically relevant CO<sub>2</sub>-induced acidification. RBC CA activity in red drum (*Sciaenops ocellatus*) was inhibited with ethoxzolamide by 53.7±0.5%, which prompted a significant reduction in O<sub>2</sub> offloading rate by 54.3±5.4% ( $P=0.0206$ , two-tailed paired *t*-test;  $n=7$ ). Conversely, a 2.03-fold increase in RBC CA activity prompted a 2.14-fold increase in O<sub>2</sub> offloading rate ( $P<0.001$ , two-tailed paired *t*-test;  $n=8$ ). This approximately 1:1 relationship between RBC CA activity and Hb-O<sub>2</sub> offloading rate coincided with a similar allometric scaling exponent for RBC CA activity and maximum metabolic rate. Together, our data suggest that RBC CA is rate limiting for O<sub>2</sub> delivery in red drum.

**KEY WORDS:** Respiratory gas exchange, Acidification, Hemoglobin, Teleosts

## INTRODUCTION

The combined climate change stressors of warming, acidification and deoxygenation are predicted to have profound impacts on fish performance and distribution (Deutsch et al., 2015; Rutterford et al., 2015). The relative resilience of fishes is thought to depend on the proliferation of existing advantageous physiological traits, or the potential of species to acclimatize via phenotypic plasticity. Importantly, ocean warming, acidification and deoxygenation are inherently respiratory stressors that have the potential to constrain O<sub>2</sub> supply capacity and thereby limit the available energy for fish to undertake ecologically important activities (Gillooly et al., 2001; Brown et al., 2004; Pörtner and Lannig, 2009; Deutsch et al., 2015; Lefevre, 2016). To properly understand the adaptive capabilities of fishes, it is imperative that we have a thorough understanding of the underlying respiratory mechanisms that limit O<sub>2</sub> supply capacity.

While the fundamental principles of respiratory gas transport in fishes are well established, recent advances have described a novel mechanism that may facilitate O<sub>2</sub> extraction at the tissues. This mechanism depends on the interplay between intracellular red blood cell pH (RBC pH<sub>i</sub>) and hemoglobin (Hb)-O<sub>2</sub> binding affinity (Fig. 1). Many teleosts possess extremely pH-sensitive Hbs (Root effect Hbs).

Unlike the Bohr effect Hbs found in most vertebrates, a decrease in pH<sub>i</sub> affects the affinity and capacity of Hb-O<sub>2</sub> binding, even at high O<sub>2</sub> tensions (Root, 1931; Pelster and Weber, 1991). To protect O<sub>2</sub> uptake at the gills, the adoption of pH-sensitive Root effect Hbs is often accompanied by β-adrenergic Na<sup>+</sup>/H<sup>+</sup> exchangers (β-NHEs) that remove H<sup>+</sup> from the intracellular space during periods of stress (e.g. exercise) (Nikinmaa et al., 1990; Berenbrink et al., 2005). However, recent studies suggest the presence of plasma-accessible carbonic anhydrase (paCA) at the tissues short-circuits this process. paCA generates CO<sub>2</sub> in the plasma from excreted H<sup>+</sup>, which moves back into the RBCs where it is subsequently hydrated by RBC carbonic anhydrase (CA). This creates greater intracellular acidification, which decreases Hb-O<sub>2</sub> binding affinity/capacity, and more O<sub>2</sub> is offloaded from Hb (Rummer and Brauner, 2011; Randall et al., 2014; Alderman et al., 2016; Harter et al., 2019; Nikinmaa et al., 2019).

In this unique model of O<sub>2</sub> transport, the Root effect and thus O<sub>2</sub> delivery are dependent on the rate of intracellular acidification, yet the importance of RBC CA has been overlooked. RBC CA is generally thought of as a CO<sub>2</sub> transport enzyme that is present well in excess for any known physiological function (Swenson and Maren, 1978; Perry, 1986). Maren and Swenson (1980) originally hypothesized that RBC CA may influence O<sub>2</sub> delivery in vertebrates by defining the rate of RBC acidification and subsequent O<sub>2</sub> offloading via the Bohr effect. Complete RBC CA inhibition decreased O<sub>2</sub> offloading to 10–40% of its original magnitude, but the authors concluded that RBC CA activity was present well in excess of that required for normal O<sub>2</sub> delivery. However, the studied species did not possess Root effect Hbs. Recent work on a variety of fish lineages suggests that high-activity RBC CA is limited to those lineages that also possess Root effect Hbs (Dichiera et al., 2020). This prompted us to revisit the hypothesis that RBC CA activity may limit O<sub>2</sub> delivery in fishes. Here, we present biochemical and metabolic evidence supporting a role for RBC CA activity in dictating the rate of O<sub>2</sub> delivery in red drum, *Sciaenops ocellatus* (Linnaeus 1766).

## MATERIALS AND METHODS

### Animal care and handling

Fish were first sampled to determine whether the study species possessed the characteristics necessary for the proposed tissue O<sub>2</sub> delivery model. Juvenile red drum were obtained from Ekstom Aquaculture, LLC (El Campo, TX, USA) and held in 600 l tanks receiving full-strength recirculating seawater (22±2°C). Fish were sampled for whole blood under anesthesia, or for tissues after euthanasia via immersion in tricaine methanesulfonate (MS-222; 100 mg l<sup>-1</sup> for anesthesia, 250 mg l<sup>-1</sup> for euthanasia, buffered with 500 mg l<sup>-1</sup> NaHCO<sub>3</sub>). Packed RBCs were isolated for Root effect quantification ( $n=8$ ). Whole blood was collected for β-NHE activity ( $n=3$ ). Muscle and heart were collected for paCA identification ( $n=6$ ).

The University of Texas at Austin Marine Science Institute, 750 Channel View Drive, Port Aransas, TX 78373, USA.

\*Author for correspondence (angelina.dichiera@utexas.edu)

 A.M.D., 0000-0002-9635-0229; A.J.E., 0000-0002-7262-4408

Received 10 July 2020; Accepted 8 October 2020

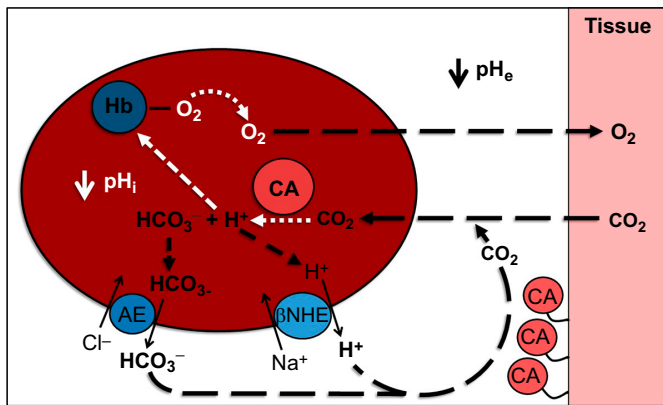


**Fig. 1. Diagram of simplified respiratory gas exchange in the red blood cell of most teleosts.** Represented within the red blood cell (RBC) are hemoglobin (Hb), RBC carbonic anhydrase (CA), β-adrenergic Na<sup>+</sup>/H<sup>+</sup> proton exchanger (β-NHE) and anion exchange protein (AE). Plasma-accessible CAs are bound to the cardiovascular tissue. In this system, described by Rummer and colleagues (Rummer and Brauner, 2011; Rummer et al., 2013; Rummer and Brauner, 2015), under acidosis wherein extracellular pH (pH<sub>e</sub>) decreases, paCA short-circuits β-NHE at the tissues to further acidify the intracellular environment and Root effect Hbs offload oxygen (O<sub>2</sub>). White arrows represent the contribution that RBC CA can make to intracellular acidification (intracellular pH, pH<sub>i</sub>), Hb-O<sub>2</sub> saturation and O<sub>2</sub> delivery to the tissue.

For O<sub>2</sub> offloading assays, adult red drum ( $n=21$ , mean±s.e.m. mass 3.06±0.21 kg) were collected via hook-and-line in Port Aransas, TX, USA (water temperature 23–31°C) and blood was sampled in the field. For RBC CA activity scaling, blood samples were used from the aforementioned wild-caught red drum and included an additional 7 wild-caught individuals whose sample volumes were too low to be used for O<sub>2</sub> offloading assays. Additional juvenile to subadult red drum obtained from Ekstom Aquaculture, LLC ( $n=15$ , mass 8.8–495 g) and adult long-term broodstock at the University of Texas Fisheries and Mariculture Laboratory ( $n=3$ , mass 7.4–9.3 kg) were sampled for whole blood under anesthesia.

All blood samples were collected via caudal puncture into a heparinized syringe, transferred to a microcentrifuge tube, and immediately put on ice. Samples were centrifuged for 2 min at 10,000 *g* to separate RBCs from plasma. Plasma was discarded, and remaining RBCs were washed 3 times with cold isotonic saline (300 mOsm l<sup>-1</sup> NaCl) to remove any remaining plasma or extracellular components. All fish were handled according to the University of Texas at Austin Institute Animal Care and Use Committee guidelines.

### Root effect verification

The blood oxygen binding system (BOBS, Loligo® Systems) was used to quantify the Root effect in red drum. Hemolysates were created with 15 μl packed RBCs (<20% methemoglobin, metHb) and 45 μl buffer solutions (100 mmol l<sup>-1</sup> Hepes and 40 mmol l<sup>-1</sup> KCl final hemolysate concentration) of different pH (6.3–8.0). We only measured metHb (i.e. Hb that cannot bind oxygen) prior to the Root effect verification (<20% metHb). However, metHb is generally low in our study species at low pH. For example, the individuals' blood sampled in the field for the O<sub>2</sub> offloading assays below had 11.19±2.01% metHb with a low pH<sub>i</sub> of 6.83±0.03 (means±s.e.m.,  $n=21$ ). The BOBS spectrophotometer was calibrated as per the manufacturer's recommendations. Samples were warmed to room temperature (22°C). The pH of each sample was taken before and after each BOBS run to ensure an accurate pH was

recorded for each hemolysate. A 1 μl sample of lysate was used for each run, and absorbance under 100% O<sub>2</sub> was measured for 3–4 min until a stable isosbestic wavelength ( $\lambda=390$  nm) and measurement wavelength ( $\lambda=436$  nm) were observed, after which the process was repeated at 0% O<sub>2</sub> (100% N<sub>2</sub>). The absolute difference between absorbance at 100% and 0% O<sub>2</sub> was calculated and represented the full scope of Hb-O<sub>2</sub> saturation (%) as compared with that at pH 8.0 (i.e. pH 8.0=100% relative saturation). Average O<sub>2</sub> binding (%) was calculated for each pH, and linearly regressed using SigmaPlot 13.0.

### β-NHE activity verification

Packed RBCs were mixed with physiological saline (150 mmol l<sup>-1</sup> NaCl, 4 mmol l<sup>-1</sup> KCl, 7 mmol l<sup>-1</sup> NaHCO<sub>3</sub>, 1.5 mmol l<sup>-1</sup> MgSO<sub>4</sub>·7H<sub>2</sub>O, 0.5 mmol l<sup>-1</sup> NaH<sub>2</sub>PO<sub>4</sub>, 1.5 mmol l<sup>-1</sup> CaCl<sub>2</sub>·2H<sub>2</sub>O; adjusted to 330 mOsm with NaCl) to 25% hematocrit. Each sample was equilibrated in a tonometer at a mean (±s.e.m.) temperature of 22±2°C with 0.5% CO<sub>2</sub>, 5% O<sub>2</sub> and 94.5% N<sub>2</sub> for 1 h. A final concentration of 10<sup>-5</sup> mol l<sup>-1</sup> isoproterenol (β-NHE agonist) was used to produce an increase in hematocrit (%) indicative of the β-NHE response (Nikinmaa, 1982; Fuchs and Albers, 1988; Caldwell et al., 2006).

### Identification of paCA

A previously obtained full-length CA IV transcript for red drum (GenBank accession number MT362925) was used to develop reverse transcription PCR (RT-PCR) primers (F 5'-GCAGTCCTTGGGTTTTCTATG-3'; R 5'-TGGTCATATTCTGCTCAGATGG-3') that produced a single 157 bp amplicon. We then verified the presence of this isoform in red drum heart and muscle template cDNA ( $n=6$  per tissue) using the following RT-PCR protocol: an initial denaturing temperature of 94°C for 2 min, 40 cycles of 94°C for 30 s, 58°C for 15 s, 72°C for 1 min, and final extension at 72°C for 5 min. Resulting PCR products were run on a 2% agarose gel and imaged using the BioRad® ChemiDoc.

### RBC CA activity measurements

RBC CA activity was measured using a modified ΔpH method (Henry, 1991) using an Orion 8102BN ROSS Combination pH electrode (Thermo Scientific). RBC samples were lysed using a 500 times dilution in deionized water. A 2 μl aliquot of each sample was added to 5 ml buffer medium (225 mmol l<sup>-1</sup> D-mannitol, 13 mmol l<sup>-1</sup> Tris base, 75 mmol l<sup>-1</sup> sucrose) held at 4°C and 200 μl of CO<sub>2</sub>-saturated distilled water (generated through constant bubbling of 5 psi CO<sub>2</sub> into distilled water held at 4°C) was injected into the medium using a Hamilton syringe. All reactions were performed in triplicate. For RBC CA inhibition and addition treatments (see below), the time for the catalyzed reaction ( $t_{\text{obs}}$ ) and the time for the uncatalyzed reaction ( $t_{\text{uncat}}$ ; reaction with no sample and CO<sub>2</sub>-saturated distilled water only) to change 0.15 pH units were calculated to determine enzyme units ( $E_0$ ).

For RBC CA activity scaling, 10 μl samples were used. The uncatalyzed reaction rate was subtracted from the observed rate to obtain the true catalyzed reaction rate. The buffer capacity (μmol H<sup>+</sup> pH unit<sup>-1</sup>) was determined prior to measurements via addition of 50 μl 0.1 mol l<sup>-1</sup> HCl to the buffer medium, then calculating the differences in initial and final pH, standardized to volume. This value was used to convert the catalyzed and uncatalyzed reaction rates from pH units min<sup>-1</sup> to μmol H<sup>+</sup> min<sup>-1</sup>. RBC CA activity was standardized by protein content (μmol H<sup>+</sup> min<sup>-1</sup> μg<sup>-1</sup> protein) measured via a Coomassie Plus™ (Bradford) Assay Kit (Thermo Scientific).

## O<sub>2</sub> offloading assays

An *in vitro* Hb-O<sub>2</sub> offloading assay was developed and modified from previous approaches (Maren and Swenson, 1980; Rummer et al., 2010). Briefly, this assay allowed us to manipulate RBC CA activity in a hemolysate, subject it to CO<sub>2</sub>-based acidification to prompt the Root effect, and then quantify the rate of O<sub>2</sub> offloading from Hb (Fig. 2). Importantly, the assay was designed to mimic *in vivo* physiological conditions, with a hemolysate pH of 6.92±0.01 (mean±s.e.m., *n*=30) and an approximate CO<sub>2</sub>-induced acidification of 0.2 pH units, which is consistent with ΔpH<sub>i</sub> following exhaustive exercise in other teleosts (Milligan and Wood, 1987).

Vertical mini respirometry chambers (Loligo® Systems) were used for all O<sub>2</sub> offloading assays. O<sub>2</sub> partial pressure (*P*<sub>O<sub>2</sub></sub>) was measured over time using a PreSens® OXY-4 mini 4-channel fiber optic O<sub>2</sub> transmitter, and data were collected using PreSens® software (OXY-4 mini version 2.30FB). We used 10% hemolysates (3 times-washed packed RBCs in 10 mmol l<sup>-1</sup> Hepes, 4 mmol l<sup>-1</sup> KCl), as preliminary experiments found 10% hemolysate provided the most quantifiable change in *P*<sub>O<sub>2</sub></sub>. All hemolysates were sonicated and snap frozen at -80°C to ensure a homogeneous solution. Prior to assay, hemolysates were equilibrated in a tonometer for 10 min and exposed to a gas mix of 79% N<sub>2</sub>:21% O<sub>2</sub> at 22°C. While CA activity assays were conducted at 4°C to decrease the reaction rate and increase the resolution of pH change for measurement, fish were sampled at 22°C; thus, O<sub>2</sub> offloading assays were run at 22°C to mimic *in vivo* conditions. We assume here that the inhibitor constant is consistent across temperatures (as per Maren and Swenson, 1980), and furthermore that the effect of temperature is consistent across the treatments.

Sealed hemolysate was then allowed to stabilize for 5 min in the assay chamber with gentle mixing. The Root effect reaction was then catalyzed by adding 200 μl of hemolysate buffer (pH 7.0) bubbled with 79% CO<sub>2</sub>:21% O<sub>2</sub> through an injection port. Note that the addition of 21% O<sub>2</sub> to the injection solution was required to prevent dilution of O<sub>2</sub> in the closed assay system. The reaction was allowed to proceed for an additional 5 min. Blank assays (i.e. buffer only) were used to validate that the injection protocol did not impact O<sub>2</sub> saturation in the assay chamber.

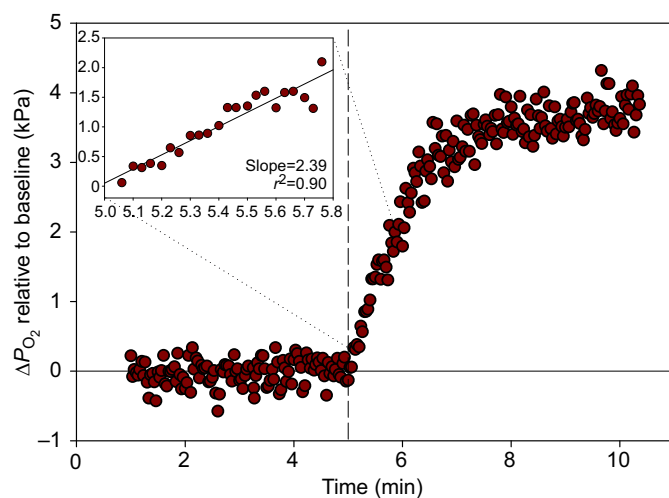


**Fig. 2. Representative trace demonstrating the change in O<sub>2</sub> partial pressure (Δ*P*<sub>O<sub>2</sub></sub>) over time following CO<sub>2</sub> injection.** *P*<sub>O<sub>2</sub></sub> was measured relative to baseline (average kPa of first 5 min). The dashed line represents the time of CO<sub>2</sub> injection at 5 min. The inset shows the slope of a change in 2 kPa O<sub>2</sub> over time, which becomes the oxygen offloading rate (Δ*P*<sub>O<sub>2</sub></sub> min<sup>-1</sup>). Trace from control sample (Fish ID 072519-1).

The first series of experiments examined the effects of the potent CA inhibitor ethoxzolamide on CO<sub>2</sub>-induced O<sub>2</sub> offloading from Hb. Hemolysates were treated with sufficient ethoxzolamide to inhibit 50% of RBC CA activity as determined by inhibitor enzyme kinetic analysis. The inhibitor constant (*K*<sub>i</sub>) of ethoxzolamide for red drum RBC CA was first determined using the Easson–Stedman method described by Maren et al. (1960). The determined *K*<sub>i</sub> (nmol l<sup>-1</sup>) was used to calculate the concentration of ethoxzolamide required to inhibit 50% of the total CA pool in each hemolysate used during the O<sub>2</sub> offloading assay. Ethoxzolamide was dissolved in 1% dimethyl sulfoxide (DMSO) for all inhibition assays, and inhibition controls were sham injected with equal amounts of DMSO prior to tonometry. Control and inhibition O<sub>2</sub> offloading assays were paired (i.e. the same blood sample) and performed in parallel.

The second series of experiments used bovine erythrocyte CA to double CA activity in the hemolysate prior to assessing CO<sub>2</sub>-induced O<sub>2</sub> offloading. For addition treatments, hemolysate CA activity was first calculated using the ΔpH method described above. CA (lyophilized powder) from bovine erythrocytes (C3934; Sigma-Aldrich) was added until repeated hemolysate CA activity assays demonstrated doubled activity. Though mammalian, the source of CA is irrelevant as we simply sought to increase the speed of the CO<sub>2</sub> hydration reaction. Addition controls were sham injected with isotonic saline (the diluent for bovine RBC CA) prior to tonometry. Control and addition O<sub>2</sub> offloading assays were paired and performed in parallel as above.

## Metabolic rate and RBC CA activity scaling

As a final test of our hypothesis, we sought to compare the allometric scaling relationship for RBC CA activity with a previously determined scaling relationship for maximum metabolic rate (MMR) in red drum. Mass-specific maximum metabolic rate (mg O<sub>2</sub> kg<sup>-1</sup> h<sup>-1</sup>) data for red drum (*n*=49, mass 0.91–99.0 g) were obtained from Ackerly and Esbaugh (2020). RBC CA activity (μmol H<sup>+</sup> min<sup>-1</sup> μg<sup>-1</sup> protein) was calculated as described above for red drum (*n*=46, mass 8.8–9300 g). Data were natural log transformed prior to regression analyses.

## Statistical analyses

SigmaPlot 13.0 was used to generate O<sub>2</sub> saturation traces from raw PreSens® software data. To standardize across treatments, raw O<sub>2</sub> offloading rate (Δ*P*<sub>O<sub>2</sub></sub> min<sup>-1</sup>) was calculated over a Δ*P*<sub>O<sub>2</sub></sub> of 2 kPa after injection of CO<sub>2</sub>. Only linear regressions (Δ*P*<sub>O<sub>2</sub></sub> min<sup>-1</sup>) where *r*<sup>2</sup>>0.75 were used for final calculations. Differences in O<sub>2</sub> offloading rates between control and treatments were evaluated with two-tailed paired *t*-tests, using α<0.05 to determine significance. Linear regressions for scaling relationships were also generated using SigmaPlot 13.0. All data are given as means±s.e.m.

## RESULTS

Hemolysate samples (*n*=35) were tested at 6 different pH values for their maximum Hb-O<sub>2</sub> saturation (%) when exposed to 100% O<sub>2</sub>. Mean (±s.e.m.) maximum Hb-O<sub>2</sub> was 100±0%, 80.08±6.94%, 76.70±4.95%, 57.14±4.43%, 44.03±4.42% and 32.56±5.70% for pH<sub>i</sub> 7.98±0.01, 7.71±0.05, 7.30±0.03, 6.93±0.05, 6.60±0.01 and 6.47±0.04, respectively. Linear regression for all samples demonstrated a clear relationship between pH and Hb-O<sub>2</sub> (%) (Fig. S1; *r*<sup>2</sup>=0.72) when subjected to 100% O<sub>2</sub>, which is indicative of Root effect Hbs. Exposure to isoproterenol (a β-NHE agonist) following incubation under hypoxic and hypercapnic conditions typically potentiates a swelling response of the RBC driven by β-NHE, which can then be measured as an increase in hematocrit

**Table 1. Calculation of red blood cell carbonic anhydrase (RBC CA) activity in the presence of inhibitor**

Fish ID	$E_0$ per 2 $\mu$ l	$E_0$ per 3.5 ml	[I] used per 35 $\mu$ l ( $10^{-4}$ mol l $^{-1}$ )	[I] total (nmol l $^{-1}$ )	$K_i$ (nmol l $^{-1}$ per $E_0$ )	RBC CA activity (%)
041019-1	8.786	15,375.80	2.25	2250	0.1463	52.48
041019-2	7.585	13,273.70	2	2000	0.1507	53.12
041019-4	8.752	15,315.26	2.25	2250	0.1470	54.88
072519-2	14.715	25,751.30	4	4000	0.1553	53.79
072519-3	12.288	21,504.69	3.5	3500	0.1628	54.82
072519-4	10.536	18,437.91	3	3000	0.1627	54.81
081419-1	5.940	10,395.02	1.5	1500	0.1443	52.18

Percentage activity following inhibition was based on estimated RBC CA activity (where control=100%) using the calculated inhibitor constant  $K_i$  ( $[I]/E_0$ , where  $[I]$  is the concentration of inhibitor and  $E_0$  represents enzyme units) and the logarithmic relationship between ethoxzolamide concentration and percentage inhibition of activity (Fig. S4).

over time. In red drum, this response was strong enough to result in RBC lysis, which occurred in all isoproterenol samples within the 60 min assay (Table S1;  $n=3$ ). RT-PCR and gel imaging demonstrated positive signals for paCA (157 bp) in both the heart and muscle tissue (Fig. S2).

Average calculations for  $1/(1-i)$  and  $[I]/i$  (where  $[I]$  is total inhibitor concentration and  $i$  is calculated fractional inhibition) for nine ethoxzolamide concentrations (0.02–1 nmol l $^{-1}$ ) were used to create an Easson–Stedman plot via linear regression (Table S2, Fig. S3). The plot showed a strong positive linear relationship ( $r^2=0.95$ ). Importantly, the slope of this line ( $m=0.152$ ) represents the concentration of ethoxzolamide (nmol l $^{-1}$ ) necessary to inhibit 50% of RBC CA activity per  $E_0$ . These data were also used to establish the logarithmic relationship between average percentage inhibition and ethoxzolamide concentration ( $y=21.92\ln x+94.63$ ). This was then used to estimate the percentage inhibition of RBC CA activity according to the ethoxzolamide concentration added to each sample in the inhibition treatment (Table 1; Fig. S4).

The average RBC CA activity in the presence of inhibitor was inhibited by  $53.7\pm 0.5\%$  ( $n=7$ ) relative to control. The average control  $O_2$  offloading rate was  $4.55\pm 1.13 \Delta P_{O_2} \text{ min}^{-1}$  following addition of  $CO_2$ , and the average offloading rate with CA inhibition was  $1.78\pm 0.25 \Delta P_{O_2} \text{ min}^{-1}$  (Table 2, Fig. 3A;  $P=0.0206$ , two-tailed paired  $t$ -test;  $n=7$ ). This equated to a significant inhibition of  $O_2$  offloading rate by  $54.3\pm 5.4\%$ . For the hemolysates following CA addition, average CA activity was increased 2.03-fold relative to controls (Table 3;  $n=8$ ). Control  $O_2$  offloading rate was

$4.70\pm 0.62 \Delta P_{O_2} \text{ min}^{-1}$ , and following addition of CA increased to  $9.75\pm 1.03 \Delta P_{O_2} \text{ min}^{-1}$  (Table 4, Fig. 3B;  $P<0.001$ , two-tailed paired  $t$ -test;  $n=8$ ). When paired, the average  $O_2$  offloading rate was significantly increased 2.14-fold relative to controls.

Linear regression analyses demonstrated significant negative linear relationships whereby MMR and RBC CA activity decreased with increases in mass (Fig. 4;  $P<0.001$  for each).  $r^2$  values were 0.78 and 0.62, respectively. Importantly, the slopes of each regression were similar ( $-0.20$  and  $-0.19$ , respectively), which suggests a similar rate of change across body size for both MMR and RBC CA activity.

## DISCUSSION

To revisit the hypothesis that RBC CA activity may limit  $O_2$  delivery in fishes, we first had to determine whether red drum possessed the necessary characteristics for the proposed tissue  $O_2$  delivery model: Root effect Hbs, RBC  $\beta$ -NHE activity and plasma-accessible CA in aerobically demanding tissues. Red drum Hbs show a strong relationship with pH and binding capacity at 100% environmental  $O_2$ . RBCs lysed in the presence of a  $\beta$ -NHE agonist, a response more robust than the typical swelling response observed in other teleosts (Nikinmaa, 1982; Fuchs and Albers, 1988; Caldwell et al., 2006). As the purpose was simply to validate that red drum did in fact possess a  $\beta$ -NHE response, both swelling and the resulting cell lysis were taken as confirmation. Aerobic tissues (heart and muscle) demonstrated the presence of paCA. While we were not able to validate the localization of this protein in the heart,

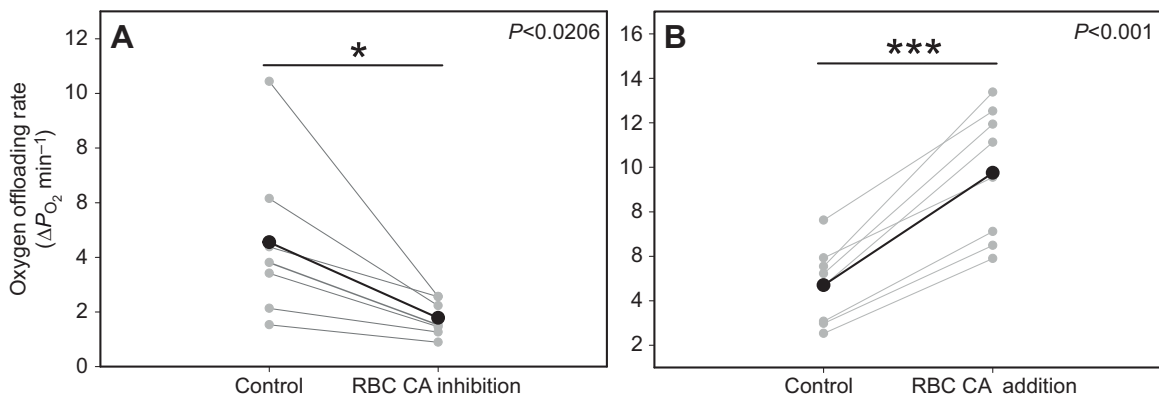


**Fig. 3. Effect of RBC CA inhibition and CA addition on oxygen offloading rate relative to control.** (A) RBC CA inhibition significantly decreased oxygen offloading rate by 54% relative to control ( $P=0.0206$ , two-tailed paired  $t$ -test,  $n=7$ ). (B) RBC CA addition significantly increased oxygen offloading rate by 2.14-fold relative to control ( $P<0.001$ , two-tailed paired  $t$ -test,  $n=8$ ). Each control hemolysate was paired with its respective treatment hemolysate from the same individual, represented by the gray dots connected with gray lines. Average oxygen offloading rates for controls and their respective treatments are represented by the black dots connected with black lines. Fish ID 081419-1 (control and inhibition sample, see Table 2 for data) did not affect the statistical significance when removed from the dataset ( $P=0.0104$ , two-tailed paired  $t$ -test,  $n=6$ ), and therefore was kept for transparency.

**Table 2. Comparison of O<sub>2</sub> offloading rate with estimated RBC CA activity following CA inhibition**

Fish ID	O <sub>2</sub> offloading rate ( $\Delta P_{O_2}$ min <sup>-1</sup> )		O <sub>2</sub> offloading rate inhibited (%)	RBC CA activity inhibited (%)
	Control	CA inhibition		
041019-1	3.41	1.46	57.25	52.48
041019-2	3.81	1.52	59.96	53.12
041019-4	1.52	0.89	41.58	54.88
072519-2	2.13	1.27	40.53	53.79
072519-3	6.15	2.23	63.75	54.82
072519-4	4.38	2.56	41.61	54.81
081419-1	10.43	2.56	75.44	52.18
Mean±s.e.m.	4.55±1.13	1.78±0.25	54.30±5.38	53.73±0.47

O<sub>2</sub> offloading rate was based on respirometry measurements and RBC CA activity was calculated as in Table 1 ( $n=7$ ). Offloading rate and RBC activity following CA inhibition are given as a percentage relative to control values.

presumably it is located in the lumen as described in other fish (Rummer and Brauner, 2011; Alderman et al., 2016; Harter et al., 2019). Red drum thus possess all the necessary characteristics for the proposed tissue O<sub>2</sub> delivery mechanism: Root effect Hbs,  $\beta$ -NHE, paCA and high-activity RBC CA.

We first predicted that if RBC CA activity was rate limiting for O<sub>2</sub> delivery then inhibition of RBC CA activity would reduce *in vitro* the rate of O<sub>2</sub> offloading from Hb. The close association between the magnitude of inhibition for both RBC CA activity and O<sub>2</sub> offloading rate following ethoxzolamide treatment is consistent with a role for RBC CA in mediating O<sub>2</sub> delivery. More simply, the data suggest that RBC CA inhibition results in a similar decline in the rate at which O<sub>2</sub> dissociates from Hb via the Root effect. We further tested our hypothesis by adding sufficient bovine RBC CA to the hemolysate to double total CA activity, with the prediction that we would observe an increase in O<sub>2</sub> offloading rate. Importantly, if RBC CA activity was in excess of that needed for O<sub>2</sub> delivery under normal conditions then addition of CA to the hemolysate would have no effect on the observed rate of O<sub>2</sub> offloading. As such, these data provide strong support for the hypothesis that high-activity RBC CA is rate limiting for O<sub>2</sub> delivery in fishes with characteristics for enhanced tissue O<sub>2</sub> delivery. It is also important to note that the observed changes in O<sub>2</sub> offloading rate between treatments and experiments was not the product of different degrees of CO<sub>2</sub>-induced acidification. There was no significant difference in the final  $\Delta$ pH across treatments (Fig. 5;  $P=0.375$ , one-way ANOVA on ranks), nor was O<sub>2</sub> offloading rate correlated with  $\Delta$ pH (data not shown). This verifies that the total

**Table 3. Calculation of RBC CA activity following addition of CA**

Fish ID	$E_0$		Increase in RBC CA activity
	Control	CA addition	
081419-1	10,395.02	26,907.55	2.59
081419-2	19,232.71	35,323.61	1.84
082919-1	31,346.78	75,226.77	2.40
082919-5	26,139.85	52,854.98	2.02
091719-1	24,758.78	45,018.21	1.82
091719-2	25,863.35	44,859.73	1.73
091719-4	20,329.66	37,562.49	1.85
091719-5	18,119.01	35,469.50	1.96

Enzyme units ( $E_0$ ) in control and following addition of CA were calculated using the electrometric  $\Delta$ pH method (Henry, 1991). Calculation of the increase in RBC CA activity following CA addition was based on the increase in  $E_0$ , and data represent a fold-change.

**Table 4. Comparison of O<sub>2</sub> offloading rate with estimated RBC CA activity following addition of CA**

Fish ID	O <sub>2</sub> offloading rate ( $\Delta P_{O_2}$ min <sup>-1</sup> )		Increase in O <sub>2</sub> offloading rate	Increase in RBC CA activity
	Control	CA addition		
081419-1	7.62	12.52	1.64	2.59
081419-2	2.98	6.49	2.18	1.84
082919-1	5.92	9.55	1.61	2.40
082919-5	4.68	11.12	2.38	2.02
091719-1	5.54	13.38	2.41	1.82
091719-2	2.53	5.90	2.33	1.73
091719-4	5.21	11.93	2.29	1.85
091719-5	3.07	7.11	2.31	1.96
Mean±s.e.m.	4.70±0.62	9.75±1.03	2.14±0.12	2.03±0.11

O<sub>2</sub> offloading rate was based on respirometry measurements and RBC CA activity was calculated as in Table 3. Data represent the fold-change following addition of CA ( $n=8$ ).

acidification load was consistent and indicates  $\Delta$ pH had no effect on the changes we saw in O<sub>2</sub> offloading rates across treatments.

For our inhibition treatment, RBC CA activity decreased by 54% relative to control and we observed a 54% decrease in average O<sub>2</sub> offloading rate relative to control. Conversely, in our addition treatment, CA activity increased by 2.03-fold and the O<sub>2</sub> offloading rate increased by 2.14-fold. This approximately 1:1 relationship stands in stark contrast to previous work on a range of vertebrates with Bohr effect Hbs, whereby a 23- to 360-fold excess of CA activity was present beyond that required to maintain normal O<sub>2</sub> offloading rates via the Bohr effect (Maren and Swenson, 1980). While this study was focused on a single teleost species, it is important to note that these results are also consistent with our previous work that suggested co-evolution of high-activity RBC CA activity and the Root effect across an array of fish lineages. Most notably, elasmobranchs and hagfishes that lack a Root effect also lack high-activity RBC CA (Dichiera et al., 2020). While future study is clearly needed to definitively state that the results here apply to a broader array of teleosts, it seems reasonable to suggest that they will extend to those teleosts that rely on  $\beta$ -NHE short-circuiting mechanisms to enhance O<sub>2</sub> delivery via the Root effect (e.g. salmonids: Alderman et al., 2016; Harter and Brauner, 2017; Harter et al., 2019).

While the *in vitro* assay data are convincing, it is more challenging to assess the implications of high-activity RBC CA on organismal performance. This is simply because it is challenging to inhibit RBC CA activity without also inhibiting tissue CA activity and CO<sub>2</sub> transport. Similar confounding factors arise under conditions of experimental anemia, as this would alter blood O<sub>2</sub> carrying capacity and the blood Hb concentration. Instead, we chose to address the whole-animal implications by exploring the allometric relationships between RBC CA activity and O<sub>2</sub> supply capacity (i.e. MMR) as a consequence of body size. Consistent with our hypothesis that RBC CA is rate limiting for O<sub>2</sub> delivery, RBC CA activity and mass-specific MMR had similar allometric scaling patterns, suggesting a similar rate of change across body size for each parameter. While traditional allometric scaling relationships show an increase in metabolic rate with mass (scaling exponent  $\sim 0.67$ ; Schmidt-Nielsen, 1975), by using mass-specific metabolic rate here, we were able to overcome confounding factors related to the change of gas transport efficiency with size, which are well established in fish (Nilsson and Östlund-Nilsson, 2008). Smaller fish consume more O<sub>2</sub> per gram of body mass and also have higher

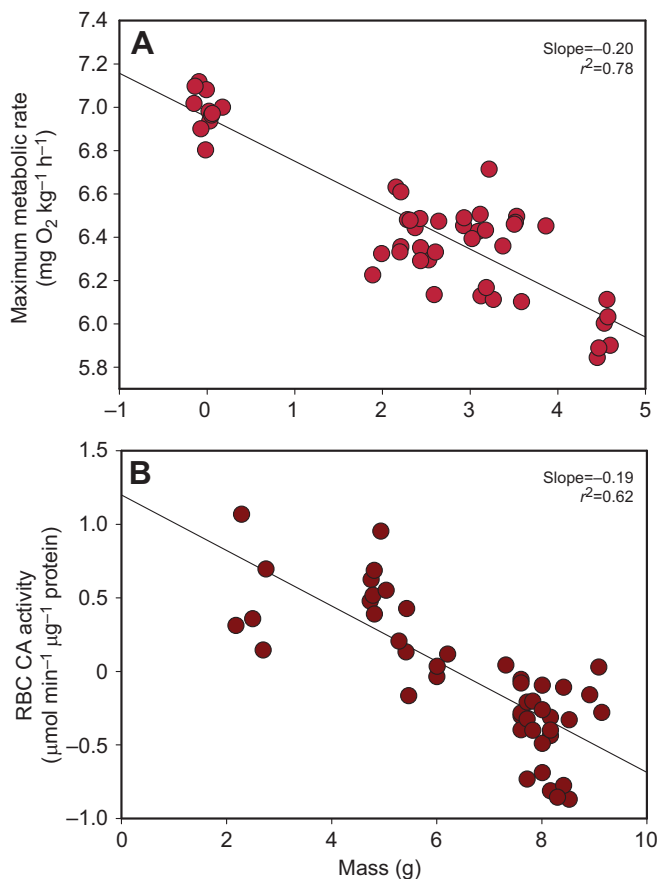


**Fig. 4. Scaling of maximum metabolic rate (MMR) and RBC CA activity with mass.** MMR (A), RBC CA activity (B) and mass were natural log transformed prior to regression analyses; MMR is mass specific. The slope represents the scaling exponent, which for MMR and RBC CA activity was  $-0.20$  and  $-0.19$ , respectively. Both MMR and RBC CA activity decreased with increases in mass. Linear regressions were significant ( $P < 0.001$ ).

RBC CA activity, which theoretically increases the speed of  $O_2$  diffusion by increasing capillary  $O_2$  tension. As MMR and aerobic scope are thought to be major determinants of ecological success – representing the capacity for reproduction, activity and growth (Priede, 1985; Burton et al., 2011) – the significance of the relationship between RBC CA and  $O_2$  consumption and offloading rate is clear. Alderman et al. (2016) previously suggested that individual variation in heart paCA activity could potentially contribute to observed differences in fitness within salmon populations (Eliason et al., 2011; Eliason et al., 2013). Likewise, RBC CA activity could potentially be developed as a non-lethal means to understand interindividual variation in aerobic capacity.

This work contributes to recent advances in fish respiratory physiology (Berenbrink et al., 2005; Rummer and Brauner, 2011; Rummer et al., 2013; Randall et al., 2014; Rummer and Brauner, 2015; Alderman et al., 2016; Brauner and Harter, 2017; Harter and Brauner, 2017; Harter et al., 2018; Harter et al., 2019; Nikinmaa et al., 2019) that jointly describe a complex mechanism by which fish maximize the acidifying potential of metabolically produced  $CO_2$  to drive  $O_2$  delivery in the tissues. Indeed, the evolutionary success of the teleost lineage is largely due to physiological adaptations that enhance tissue  $O_2$  delivery. Primarily, pH-sensitive Hbs, pH<sub>i</sub> regulatory capabilities and beneficial localization of CA are thought to dictate the ability to transport  $O_2$  (Rummer and Brauner, 2011; Rummer et al., 2013; Randall et al., 2014; Alderman et al., 2016;

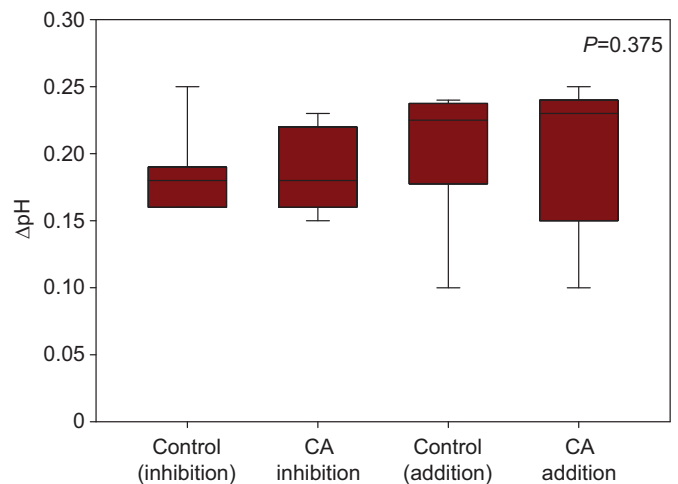


**Fig. 5.  $\Delta pH$  generated by  $CO_2$  injection across treatments.** Box and whisker plot shows the 50th percentile of  $\Delta pH$  for each treatment group; error bars denote the 10th and 90th percentiles, and the median for each treatment is represented by the line within each box. The lack of a significant difference in  $\Delta pH$  across treatments demonstrates total acidification load was consistent and  $\Delta pH$  had no effect on the changes seen in  $O_2$  offloading rates across treatments ( $P = 0.375$ , one-way ANOVA on ranks).

Harter and Brauner, 2017; Harter et al., 2018; Harter et al., 2019; Nikinmaa et al., 2019). In early-diverging fish, paCA at the gills allows for plasma-based  $CO_2$  excretion; without Root effect Hbs or  $\beta$ -NHE,  $O_2$  delivery and  $CO_2$  excretion are compartmentalized separately. RBC-mediated  $CO_2$  excretion and the pressure for high-activity RBC CA is greatly reduced, thus early-diverging species tend to possess low-activity RBC CA (McMillan et al., 2019; Dichiera et al., 2020). With teleost species that lack branchial paCA but possess high-activity RBC CA, we see the emergence of these enhanced tissue  $O_2$  delivery characteristics.

Importantly, we have framed our interpretation of the function of RBC CA in the context of recent models of pH-induced  $O_2$  delivery in fishes – models where Root effect Hb,  $\beta$ -NHE and paCA are thought to play central roles in enhanced  $O_2$  delivery in the muscle and heart (Rummer and Brauner, 2011; Rummer et al., 2013; Rummer and Brauner, 2015; Harter et al., 2019). But it is important to note that RBC CA would also contribute to the original role proposed for Root effect Hb: $O_2$  delivery to the eye and swimbladder via countercurrent rete systems. Berenbrink (2007) proposed that the Root effect was selected for in species with a choroid rete mirabile. Indeed, the relationship between retinal morphology and the magnitude of the Root effect is so strong that Damsgaard et al. (2019) suggested secondary losses of  $O_2$  secretion via a reduced Root effect may have resulted from relaxed selection on vision. More recently, Damsgaard et al. (2020) demonstrated an advanced  $O_2$  delivery mechanism in the eye, whereby vacuolar-type  $H^+$ -ATPase (VHA) and paCA work together to promote RBC acidification. Supporting our proposed role for RBC CA in  $O_2$  delivery via the Root effect, the authors observed that while specific paCA inhibition decreased choroidal  $P_{O_2}$  by nearly 60%, acetazolamide (a strong membrane-permeable CA inhibitor) inhibited choroidal  $P_{O_2}$  by >95%. The systems described for both aerobic muscles and the eye maximize  $O_2$  delivery by capitalizing on the relationship between RBC CA and Root effect Hbs. This short-circuiting action works by providing RBC CA with a higher amount of substrate for  $CO_2$  dehydration. RBC CA drives the increase in protons within the cell, directly reducing Hb- $O_2$  binding capacity and

O<sub>2</sub> offloading. While paCA has recently become a prominent mechanistic link in defining O<sub>2</sub> extraction efficiency, RBC CA seems equally crucial to the integrated process of O<sub>2</sub> delivery. Our study suggests enhanced O<sub>2</sub> delivery is driven by (1) RBC β-NHE, (2) paCA, (3) Root effect Hbs and (4) high-activity RBC CA. Furthermore, this work provides the first evidence of a rate-limiting role, and thus selective pressure, for RBC CA – an enzyme that heretofore had been considered well in excess for any physiological function in vertebrates.

#### Acknowledgements

The authors would like to thank the anonymous reviewers for their constructive comments, as well as K. L. Ackerly for metabolic rate data, and everyone who kindly helped obtain blood samples: L. M. Martin, A. J. Khursigara, B. Negrete, Jr, K. L. Ackerly and J. K. Lonhair.

#### Competing interests

The authors declare no competing or financial interests.

#### Author contributions

Conceptualization: A.J.E.; Methodology: A.M.D., A.J.E.; Formal analysis: A.M.D.; Investigation: A.M.D.; Writing - original draft: A.M.D.; Writing - review & editing: A.M.D., A.J.E.; Visualization: A.M.D.; Supervision: A.J.E.

#### Funding

This work was funded through a National Science Foundation grant (award 2002549) to A.J.E.

#### Supplementary information

Supplementary information available online at <https://jeb.biologists.org/lookup/doi/10.1242/jeb.232991.supplemental>

#### References

- Ackerly, K. L. and Esbaugh, A. J. (2020). The additive effects of oil exposure and hypoxia on aerobic performance in red drum (*Sciaenops ocellatus*). *Sci. Total Environ.* **737**, 140174. doi:10.1016/j.scitotenv.2020.140174
- Alderman, S. L., Harter, T. S., Wilson, J. M., Supuran, C. T., Farrell, A. P. and Brauner, C. J. (2016). Evidence for a plasma-accessible carbonic anhydrase in the lumen of salmon heart that may enhance oxygen delivery to the myocardium. *J. Exp. Biol.* **219**, 719–724. doi:10.1242/jeb.130443
- Berenbrink, M. (2007). Historical reconstructions of evolving physiological complexity: O<sub>2</sub> secretion in the eye and swimbladder of fishes. *J. Exp. Biol.* **210**, 1641–1652. doi:10.1242/jeb.003319
- Berenbrink, M., Koldkjær, P., Kepp, O. and Cossins, A. R. (2005). Evolution of oxygen secretion in fishes and the emergence of a complex physiological system. *Science* **307**, 1752–1757. doi:10.1126/science.1107793
- Brauner, C. J. and Harter, T. S. (2017). Beyond just hemoglobin: red blood cell potentiation of hemoglobin-oxygen unloading in fish. *J. Appl. Physiol.* **123**, 935–941. doi:10.1152/jappphysiol.00114.2017
- Brown, J. H., Gillooly, J. F., Allen, A. P., Savage, V. M. and West, G. B. (2004). Toward a metabolic theory of ecology. *Ecology* **85**, 1771–1789. doi:10.1890/03-9000
- Burton, T., Killen, S. S., Armstrong, J. D. and Metcalfe, N. B. (2011). What causes intraspecific variation in resting metabolic rate and what are its ecological consequences? *Proc. R. Soc. B* **278**, 3465–3473. doi:10.1098/rspb.2011.1778
- Caldwell, S., Rummer, J. L. and Brauner, C. J. (2006). Blood sampling techniques and storage duration: effects on the presence and magnitude of the red blood cell β-adrenergic response in rainbow trout (*Oncorhynchus mykiss*). *Comp. Biochem. Physiol. A Mol. Integr. Physiol.* **144**, 188–195. doi:10.1016/j.cbpa.2006.02.029
- Damsgaard, C., Lauridsen, H., Funder, A. M. D., Thomsen, J. S., Desvignes, T., Crossley, D. A., II, Møller, P. R., Huong, D. T. T., Phuong, N. T. and Detrich, H. W., III. (2019). Retinal oxygen supply shaped the functional evolution of the vertebrate eye. *eLife* **8**, e52153. doi:10.7554/eLife.52153
- Damsgaard, C., Lauridsen, H., Harter, T. S., Kwan, G. T., Thomsen, J. S., Funder, A. M. D., Supuran, C. T., Tresguerres, M., Matthews, P. G. D. and Brauner, C. J. (2020). A novel acidification mechanism for greatly enhanced oxygen supply to the fish retina. *eLife* **9**, e58995. doi:10.7554/eLife.58995
- Deutsch, C., Ferrel, A., Seibel, B., Pörtner, H.-O. and Huey, R. B. (2015). Climate change tightens a metabolic constraint on marine habitats. *Science* **348**, 1132–1135. doi:10.1126/science.aaa1605
- Dichiera, A. M., McMillan, O. J., Clifford, A. M., Goss, G. G., Brauner, C. J. and Esbaugh, A. J. (2020). The importance of a single amino acid substitution in reduced red blood cell carbonic anhydrase function of early-diverging fish. *J. Comp. Physiol. B* **190**, 287–296. doi:10.1007/s00360-020-01270-9
- Eliason, E. J., Clark, T. D., Hague, M. J., Hanson, L. M., Gallagher, Z. S., Jeffries, K. M., Gale, M. K., Patterson, D. A., Hinch, S. G. and Farrell, A. P. (2011). Differences in thermal tolerance among sockeye salmon populations. *Science* **332**, 109–112. doi:10.1126/science.1199158
- Eliason, E. J., Clark, T. D., Hinch, S. G. and Farrell, A. P. (2013). Cardiorespiratory collapse at high temperature in swimming adult sockeye salmon. *Conservation Physiology* **1**, cot008. doi:10.1093/conphys/cot008
- Fuchs, D. and Albers, C. (1988). Effect of adrenaline and blood gas conditions on red cell volume and intra-erythrocytic electrolytes in the carp, *Cyprinus carpio*. *J. Exp. Biol.* **137**, 457–476.
- Gillooly, J. F., Brown, J. H., West, G. B., Savage, V. M. and Charnov, E. L. (2001). Effects of size and temperature on metabolic rate. *Science* **293**, 2248–2251. doi:10.1126/science.1061967
- Harter, T. S. and Brauner, C. J. (2017). The O<sub>2</sub> and CO<sub>2</sub> transport system in teleosts and the specialized mechanisms that enhance Hb–O<sub>2</sub> unloading to tissues. *Fish Physiol.* **36**, 1–106. doi:10.1016/bs.fp.2017.09.001
- Harter, T. S., May, A. G., Federspiel, W. J., Supuran, C. T. and Brauner, C. J. (2018). Time course of red blood cell intracellular pH recovery following short-circuiting in relation to venous transit times in rainbow trout, *Oncorhynchus mykiss*. *Am. J. Physiol. Regul. Integr. Comp. Physiol.* **315**, R397–R407. doi:10.1152/ajpregu.00062.2018
- Harter, T. S., Zanuzzo, F. S., Supuran, C. T., Gamperl, A. K. and Brauner, C. J. (2019). Functional support for a novel mechanism that enhances tissue oxygen extraction in a teleost fish. *Proc. R. Soc. B* **286**, 20190339. doi:10.1098/rspb.2019.0339
- Henry, R. P. (1991). Techniques for measuring carbonic anhydrase activity in vitro. In *The Carbonic Anhydrases* (ed. S. J. Dodgson, R. E. Tashian, G. Gros and N. D. Carter), pp. 119–125. Springer. doi:10.1007/978-1-4899-0750-9\_8
- Lefevre, S. (2016). Are global warming and ocean acidification conspiring against marine ectotherms? A meta-analysis of the respiratory effects of elevated temperature, high CO<sub>2</sub> and their interaction. *Conserv. Physiol.* **4**, cow009. doi:10.1093/conphys/cow009
- Maren, T. H. and Swenson, E. R. (1980). A comparative study of the kinetics of the Bohr effect in vertebrates. *J. Physiol.* **303**, 535–547. doi:10.1113/jphysiol.1980.sp013302
- Maren, T. H., Parcell, A. L. and Malik, M. N. (1960). A kinetic analysis of carbonic anhydrase inhibition. *J. Pharmacol. Exp. Ther.* **130**, 389–400.
- McMillan, O. J. L., Dichiera, A. M., Harter, T. S., Wilson, J. M., Esbaugh, A. J. and Brauner, C. J. (2019). Blood and gill carbonic anhydrase in the context of a chondrichthyan model of CO<sub>2</sub> excretion. *Physiol. Biochem. Zool.* **92**, 554–566. doi:10.1086/705402
- Milligan, C. L. and Wood, C. M. (1987). Regulation of blood oxygen transport and red cell pH after exhaustive activity in rainbow trout (*Salmo gairdneri*) and starry flounder (*Platichthys stellatus*). *J. Exp. Biol.* **133**, 263–282.
- Nikinmaa, M. (1982). Effects of adrenaline on red cell volume and concentration gradient of protons across the red cell membrane in the rainbow trout, *Salmo gairdneri*. *Mol. Physiol.* **2**, 287–297.
- Nikinmaa, M., Tiitonen, K. and Paajaste, M. (1990). Adrenergic control of red cell pH in salmonid fish: roles of the sodium/proton exchange, Jacobs-Stewart cycle and membrane potential. *J. Exp. Biol.* **154**, 257–271.
- Nikinmaa, M., Berenbrink, M. and Brauner, C. J. (2019). Regulation of erythrocyte function: multiple evolutionary solutions for respiratory gas transport and its regulation in fish. *Acta Physiol.* **227**, e13299. doi:10.1111/apha.13299
- Nilsson, G. E. and Östlund-Nilsson, S. (2008). Does size matter for hypoxia tolerance in fish? *Biol. Rev.* **83**, 173–189. doi:10.1111/j.1469-185X.2008.00038.x
- Pelster, B. and Weber, R. (1991). The physiology of the Root effect. In *Advances in Comparative and Environmental Physiology*, vol. 8. Springer. [https://doi.org/10.1007/978-3-642-75900-0\\_2](https://doi.org/10.1007/978-3-642-75900-0_2)
- Perry, S. F. (1986). Carbon dioxide excretion in fishes. *Can. J. Zool.* **64**, 565–572. doi:10.1139/z86-083
- Pörtner, H. O. and Lannig, G. (2009). Oxygen and capacity limited thermal tolerance. *Fish Physiol.* **27**, 143–191. doi:10.1016/S1546-5098(08)00004-6
- Priede, I. G. (1985). Metabolic scope in fishes. In *Fish Energetics* (ed. P. Tytler and P. Calow), pp. 33–64. Springer. doi:10.1007/978-94-011-7918-8\_2
- Randall, D. J., Rummer, J. L., Wilson, J. M., Wang, S. and Brauner, C. J. (2014). A unique mode of tissue oxygenation and the adaptive radiation of teleost fishes. *J. Exp. Biol.* **217**, 1205–1214. doi:10.1242/jeb.093526
- Root, R. W. (1931). The respiratory function of the blood of marine fishes. *Biol. Bull.* **61**, 427–456. doi:10.2307/1536959
- Rummer, J. L. and Brauner, C. J. (2011). Plasma-accessible carbonic anhydrase at the tissue of a teleost fish may greatly enhance oxygen delivery: in vitro evidence in rainbow trout, *Oncorhynchus mykiss*. *J. Exp. Biol.* **214**, 2319–2328. doi:10.1242/jeb.054049
- Rummer, J. L. and Brauner, C. J. (2015). Root effect haemoglobins in fish may greatly enhance general oxygen delivery relative to other vertebrates. *PLoS ONE* **10**, e0139477. doi:10.1371/journal.pone.0139477
- Rummer, J. L., Roshan-Moniri, M., Balfry, S. K. and Brauner, C. J. (2010). Use it or lose it? Sablefish, *Anoplopoma fimbria*, a species representing a fifth teleostean group where the βNHE associated with the red blood cell adrenergic stress

response has been secondarily lost. *J. Exp. Biol.* **213**, 1503-1512. doi:10.1242/jeb.038844

**Rummer, J. L., Mckenzie, D. J., Innocenti, A., Supuran, C. T. and Brauner, C. J.** (2013). Root effect hemoglobin may have evolved to enhance general tissue oxygen delivery. *Science* **340**, 1327-1329. doi:10.1126/science.1233692

**Rutterford, L. A., Simpson, S. D., Jennings, S., Johnson, M. P., Blanchard, J. L., Schön, P.-J., Sims, D. W., Tinker, J. and Genner, M. J.** (2015). Future fish

distributions constrained by depth in warming seas. *Nat. Clim. Change* **5**, 569. doi:10.1038/nclimate2607

**Schmidt-Nielsen, K.** (1975). Scaling in biology: the consequences of size. *J. Exp. Zool.* **194**, 287-307. doi:10.1002/jez.1401940120

**Swenson, E. R. and Maren, T. H.** (1978). A quantitative analysis of CO<sub>2</sub> transport at rest and during maximal exercise. *Respir. Physiol.* **35**, 129-159. doi:10.1016/0034-5687(78)90018-X